

# Technology of semiconductor materials sensitive to different regions of the electromagnetic radiation spectrum

**Nina P. Khuchua,<sup>1,\*</sup> Nugzar D. Dolidze,<sup>2</sup> Nodar G. Gapishvili,<sup>2</sup>  
Revaz G. Gulyaev,<sup>2</sup> Zurab V. Jibuti,<sup>2</sup> Revaz G. Melkadze<sup>1</sup> and  
Marina G. Tigishvili<sup>1</sup>**

<sup>1</sup> *Research and Production Complex (RPC) "Electron Technology", Institute of Applied Semiconductor Technology, Iv. Javakhishvili State University, Tbilisi, Georgia*

<sup>2</sup> *Institute of Micro- and Nanoelectronics, Tbilisi, Georgia*

Ion implantation (II) of impurities in a semiconductor followed by annealing belongs to the modern techniques that make it possible to modify the fundamental properties of a material, including optical ones, due to the formation of a great number of defects. It is an important factor for the creation of electromagnetic radiation (EMR) detectors. In the present work, in order to develop EMR detectors p–n type semiconductor structures have been fabricated and studied. The p-layer was formed by implanting boron into commercial single-crystal n-type silicon at different doses ( $1 \times 10^{13}$ – $7.8 \times 10^{14} \text{ cm}^{-2}$ ) with an acceleration energy of 50 keV and subsequent annealing at 800, 900 and 1000 °C for 20 min. Diode structures have been fabricated, current–voltage characteristics have been measured and the material sensitivity to EMR of different wavelengths has been studied. It has been shown that the ion-implanted material exhibits a well-marked photosensitivity in one of the most interesting IR (1.4–2.2 μm) and UV (0.2–0.4 μm) regions. Sensitivity to X-ray exposure has also been revealed. For interpretation of the results, the idea of the appearance of defects as clusters (nanoformations) in the silicon matrix is used. The novelty of the work is both in the experimental results and in the approach “from photosensitivity spectra to defect formation” since most other researchers concentrate their attention on the identification of defects appearing during impurity implantation in Si rather than on the optical properties of the material determined by these defects.

**Keywords:** boron ion-implanted silicon; clusters; infrared and ultraviolet regions; nanoformations; photosensitivity; X-radiation

\* Corresponding author. E-mail: ninakhuchua@mail.ru

## 1. Introduction

Interest in the study of the absorption of electromagnetic radiation (EMR) by semiconductor materials in different spectral regions is growing rapidly. This is due to the ever-evolving technology of detecting devices for different ranges of infrared (IR) and ultraviolet (UV) radiation as well as for the development of X-ray sensors.

To create EMR detectors, as a rule one has to modify the fundamental properties of a semiconductor, such as band gap width, conductivity, optical transition energy, etc. One of the effective ways to do it is to form clusters in the material matrix, the size and concentration of which allow one to vary these fundamental properties.<sup>1</sup>

Obviously, in this aspect, priority can be given to ion implantation (II) of impurities into a semiconductor. Other important techniques include growing heterostructure materials by up-to-date methods of molecular beam or other types of epitaxy.

On the one hand, silicon is the basic material of modern semiconductor electronics, on the other hand, Si is transparent to wavelengths greater than 1.1 μm. Therefore, the development of effective near/mid-IR photodiodes may be facilitated, for example, by the formation of clusters/complex defects, leading to the emergence of new electronic levels.

In silicon technology, boron is a well known and widely used impurity (to obtain single-crystal p-type material, p–n junctions, etc.). However, as regards the behaviour of ion-implanted B in n-Si and, especially, the mechanism of influence of this impurity on the electrical and optical properties of the p–n structure after thermal treatment, there are many diverse and often divergent interpretations.<sup>2</sup>

At present, it has been well established that all types of point defects, such as divacancies, three-four vacancy clusters, simple (oxygen vacancy, VO) complexes, etc. are completely annealed up to 720 K.<sup>3</sup> Rapid thermal annealing at higher temperatures<sup>4</sup> engenders clusters acting as electron traps and their presence and nature depend on the annealing temperature (in the range of 700–1100 °C only two of five possible traps remain).

According to different data, extended defects can persist at annealing temperatures of about 1000 °C.<sup>5,6</sup>

During 20 keV boron implantation and annealing at 650–800 °C, only {113} defects were observed.<sup>7</sup> This suggests that dislocation loops are formed at higher temperatures, which was

<sup>1</sup> M.G. Mil'vidskii, V.V. Chaldyshev. Nanoscale atomic clusters in semiconductors as a new approach to formation of material properties. *Fizika Tekhnika Poluprov.*, vol. 32, p. 513, 1998.

<sup>2</sup> K.S. Jones, S. Prussin, E.R. Weber. A systematic analysis of defects in ion-implanted silicon. *Appl. Phys. A*, vol. 45, p. 1, 1988.

<sup>3</sup> E.g., S. Eichler, J. Gebauer, F. Börner, A. Polity, R. Krause-Rehberg, E. Wendler, B. Weber, W. Wesch, H. Börner. Defects in silicon after B<sup>+</sup> implantation: A study using a positron-beam techniques, Rutherford backscattering, secondary neutral mass-spectroscopy. *Phys. Rev. B*, vol. 56, p. 1393, 1997.

<sup>4</sup> A. Usami, M. Katayama, J. Tokuda, T. Wada. Diode characteristics and residual deep-level defects of p<sup>+</sup>–n abrupt junctions fabricated by rapid thermal annealing of boron implanted silicon. *Semicond. Sci. Technol.*, vol. 2, p. 83, 1987.

<sup>5</sup> N.A. Sobolev, A.M. Emelianov, E.I. Shek, V.I. Vdovin. Influence of post-implantation annealing on the properties of silicon light-emitting diodes obtained by boron implantation in n-Si. *Fizika Tverd. Tela*, vol. 46, p. 39, 2004.

<sup>6</sup> M.E. Law, R. Camillo-Castillo, L. Robertson, K.S. Jones. Defects in ultra-shallow junctions. In: *Defects in Microelectronic Materials and Devices*, p. 1. Boca Raton: CRC Press (2009).

<sup>7</sup> J. Liu, V. Krishnamoorthy, K.S. Jones, M.E. Law, J. Shi, T. Bennet. Transient enhanced diffusion and

confirmed by the results.<sup>8</sup> In this paper, dislocation loops of fairly large size (200–300 nm) have been found after annealing at 950 °C. Dislocation loops are described elsewhere.<sup>9–12</sup>

In an overview<sup>13</sup> it is concluded that the formation of residual extended defects in Si is of a threshold character. This means that to form these defects during thermal treatment, accumulation of a critical concentration of point defects is necessary. Here, for 10–100 keV B ions the dose should be at least  $10^{14} \text{ cm}^{-2}$ .

The presence of rather intensive luminescence in B-implanted Si is shown in refs 8–12. In ref. 14 it is assumed that intensive electroluminescence peaks can be attributed to the formation of ultranarrow (8 nm) diffusion profiles with very high B concentrations (up to  $5 \times 10^{21} \text{ cm}^{-3}$ ) containing a p-type silicon quantum well 2 nm wide. However, other authors<sup>15,16</sup> have reported the occurrence of ultrashallow p<sup>+</sup>–n junctions also during low-energy (5.5 keV) B-implantation followed by low temperature annealing.

Finally, there is little information on the photosensitivity spectra of ion-implanted silicon, especially in the IR region, and it concerns essentially other impurities. There are reports on fabrication of UV sensors,<sup>17</sup> but the physical mechanism of the effect is not discussed.

From the above and rather incomplete data it can be concluded:

1. According to the analytical review,<sup>18</sup> defect formation during ion implantation of impurities (including B) in crystalline Si and its evolution as a function of annealing have been widely investigated in the last few decades. The increasing knowledge of the features helps in the understanding of many phenomena. Nevertheless, a number of questions concerning defect agglomeration and evolution upon annealing are still unsolved.
2. Even less information exists on the mechanism of the influence of various defects on the

---

defect studies in B-implanted Si. In: *Ion Implantation Technology: Proc. 11th International Conf.*, p. 626. Austin, Texas (1996).

<sup>8</sup> M.A. Lourenco, M. Milosavljevic, G. Shao, R.M. Gwilliam, K.P. Homewood. Boron engineered dislocation loops for efficient room temperature silicon light emitting diodes. *Thin Solid Films*, vol. 504, p. 36, 2006.

<sup>9</sup> Wai Lek Ng., M.A. Lourenço, R.M. Gwilliam, S. Ledain, G. Shao, K.P. Homewood. An efficient room-temperature silicon-based light-emitting diode. *Nature*, vol. 410, p.1036, 2001.

<sup>10</sup> M.A. Green, J. Zhao, A. Wang, P.J. Reece, M. Gal. Efficient silicon light-emitting diodes. *Nature*, vol. 412, p. 805, 2001.

<sup>11</sup> A.M. Emelianov, N.A. Sobolev. Silicon light-emitting diodes with high emission power of edge luminescence. *Fizika Tekhnika Poluprov.*, vol. 42, p. 336, 2008.

<sup>12</sup> K. Frazer, D. Stowe, S. Galloway, S. Senkader, R. Falster, P. Wilshaw. The role of dislocations in producing efficient near-bandgap luminescence from silicon. *Phys. Status Solidi*, vol.4, p. 2977, 2007.

<sup>13</sup> A.R. Cheladinski, Ph.Ph. Komarov. Defect-impurity engineering in implanted silicon. *Uspekhi Fizicheskikh Nauk*, vol. 173, p. 813, 2003.

<sup>14</sup> N.T. Bagraev, L.E. Klyachkin, R.V. Kuzmin, A.M. Malyarenko, V.A. Mashkov. Infrared luminescence from silicon nanostructures heavily doped with boron. *Semiconductors*, vol. 46, p. 273, 2012.

<sup>15</sup> A. Claverie, B. Colobeau, G.B. Assayag, C. Bonafos, F. Cristiano, M. Omri, B. de Mauduit. Thermal evolution of extended defects in implanted Si: impact on dopant diffusion. *Mat. Sci. Semicond. Processing*, vol. 3, p. 269, 2000.

<sup>16</sup> C.S. Rafferty, G.H. Gilmer, M. Jaraiz, D. Eaglesham, H.-J. Grossman. Simulation of cluster evaporation and transient enhanced diffusion in silicon. *J. Appl. Phys. Lett.*, vol. 68, p. 2395, 1996.

<sup>17</sup> V. Gavrushko, A. Ionov, V. Lastkin. An improved silicon UV-photodiode obtained by As implantation. *Elektronika: Nauka, Tekhnologiya, Business*, vol. 2, p. 72, 2010.

<sup>18</sup> S. Libertino, A. La Magna. Damage formation and evolution in ion-implanted crystalline Si. Materials science with ion beams. *Topics Appl. Phys.*, vol. 116, p. 147, 2010.

optical properties of B-implanted n-type single-crystal silicon. If electroluminescence spectra are still discussed in some papers, absorption/photosensitivity spectra have been studied very poorly and are rarely related to any type of defects.

Therefore, assessment of the role of various defects arising during ion implantation of boron in silicon by studying the sensitivity of the material to different-wavelength EMR is an innovative approach, both in scientific and practical terms.

The present paper is an extension of the early studies.<sup>19</sup> Here, the implantation of B was carried out at the same energy (50 keV), but over a wider dose range ( $1 \times 10^{13}$ – $7.8 \times 10^{14}$  cm $^{-2}$ ).

The samples were annealed in the temperature range of 800–1000 °C for 20 min.

P–n diode structures have been fabricated and their sensitivity to EMR in strongly different spectral regions has been investigated.

## 2. Technology and experimental procedure

P–n structures were formed on commercial (100) n-Si wafers by II of B with doses of  $1 \times 10^{13}$ – $7.8 \times 10^{14}$  cm $^{-2}$  and an acceleration energy of 50 keV on the Vezuvi-3M implanter. The wafer resistivity was 70 Ω cm and the wafer thickness was 250 μm. The projected range,  $R_p$ , and its straggling,  $\Delta R_p$ , estimated using SRIM, were 0.1746 and 0.0557 μm, respectively. The II was followed by annealing in an argon atmosphere at temperatures of 800, 900 and 1000 °C for 20 min. Some samples were treated by pulse photon annealing (PPA) for 6 s at 1000 °C. On both sides of the ion-implanted and annealed wafer, Ti/Pt/Au contacts were formed on a Temescal setup (through an Al mask or by the lift-off photolithography technique).

The current–voltage characteristics of the samples were measured on an L2-56 semiconductor parameter analyser.

Photosensitivity spectra were recorded within the wavelength ( $\lambda$ ) range of 1–2.2 μm by standard methods using an MDR-2 monochromator with a set of filters. The photosensitivity was determined as the ratio between the open-circuit voltages for the different  $\lambda$  and for  $\lambda = 1$  μm.

The sensitivity of the samples to UV radiation was established using an LMP-4000 lamp with a typical spectrum in the 0.2–0.7 μm region. The short-circuit current was measured under two illumination conditions: with and without a UVS-1 optical filter, making it possible to select the 0.2–0.4 μm spectral region.

The current data were reduced to the illumination unit area.

The effect of X-ray radiation on the implanted structures was studied using a DRON-4 X-ray diffractometer. An cobalt X-ray tube with background radiation within 0.6–100 Å and a strong maximum at 1.7889 Å was used as the radiation source. The dependence of the short-circuit current on the dose rate was measured. To establish the X-ray radiation effect on the optical properties of the sample, photosensitivity spectra were measured immediately after irradiation and four days later. All measurements were carried out at room temperature.

---

<sup>19</sup> M.G. Tigishvili, N.G. Gapishvili, R.G. Gulyaev, Z.V. Jibuti, N.D. Dolidze, N.P. Khuchua, R.G. Melkadze. Defect engineering in technology of p-n junctions of Si. *Georgian Engineering News*, No. 4, p. 75, 2013.

### 3. Experimental results and discussion

A typical *I*-*V* characteristic of the diode taken in diffuse light is shown in Figure 1.<sup>19</sup>

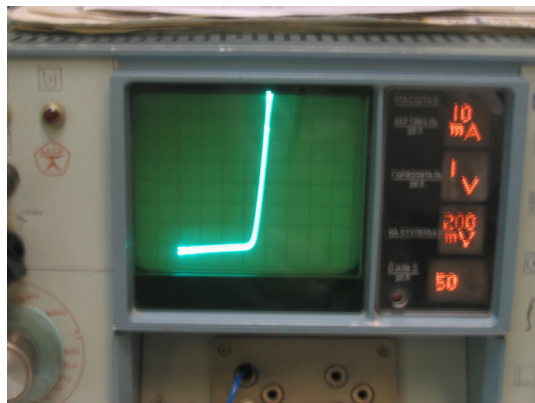


Figure 1. Typical *I*-*V* characteristic of the ion-implanted (II) sample.

Figs 2 and 3 show the IR photosensitivity spectra of the B-implanted Si samples under different implantation and annealing conditions.

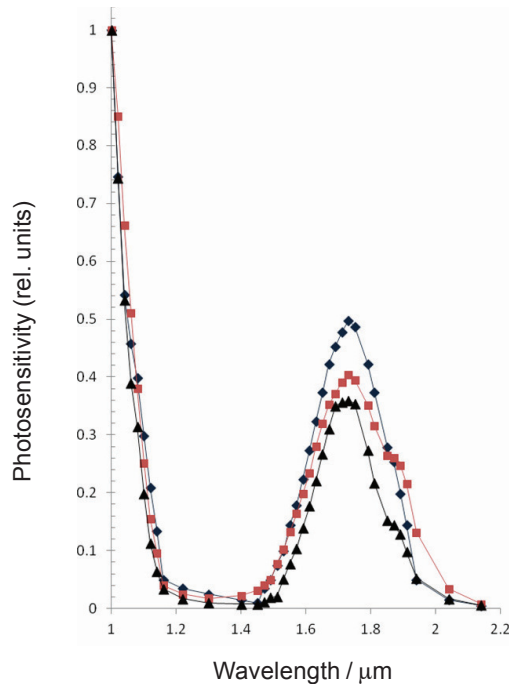


Figure 2. Photosensitivity spectra for samples implanted with different doses: ▲,  $10^{13} \text{ cm}^{-2}$ ; ■,  $10^{14} \text{ cm}^{-2}$ ; ◆,  $7.8 \times 10^{14} \text{ cm}^{-2}$  (annealing at  $1000^\circ\text{C}$  for 20 min). See legend to Fig. 3 for band labels.

As seen from Fig. 2, three high-intensity bands are observed. The band A1 lies in the short wavelength region and is related to the fundamental band-to-band absorption. Two other

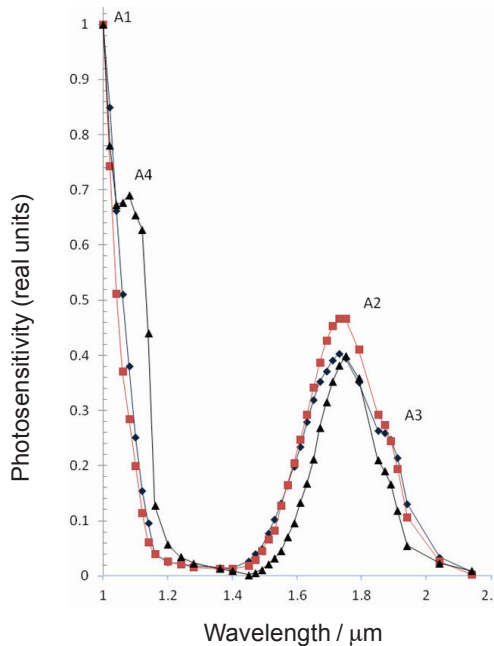


Figure 3. Photosensitivity spectra for the samples implanted with a dose of  $10^{14} \text{ cm}^{-2}$  and at different annealing temperatures: ▲, 800 °C; ■, 900 °C; ♦, 1000 °C.

bands A2 and A3 observed in the longer wavelength range (1.45–2.15 μm) are superimposed and have a distinct peak at 1.73 μm and a shoulder at longer wavelengths.

The II dose dependence of the photosensitivity is manifested in the rise of intensity of band A2 with increasing dose. As for band A3, this behaviour is clearly observed only for doses  $10^{13} \text{ cm}^{-2}$  and  $10^{14} \text{ cm}^{-2}$ . At the higher dose this band is less pronounced, which shows that for  $7.8 \times 10^{14} \text{ cm}^{-2}$  the defects responsible for the band A2 are predominant.

As seen from Fig. 3, in the spectrum of the sample annealed at 800 °C (curve 1), near the fundamental absorption edge another band (labelled A4) with a peak at 1.08 μm is observed, which disappears at higher treatment temperatures. The position of the band A2 does not depend on the annealing temperature and its intensity is maximal at 900 °C.

In Figs 2 and 3, a certain dependence of the total bandwidth of A2 and A3 on technological conditions is observed. So, at the dose of  $10^{13} \text{ cm}^{-2}$  the width is minimal, then with dose increasing it increases and again is narrowed. As for the annealing temperature effect on the total bandwidth, it is maximal at 900 °C.

In Fig. 4, the photoresponse spectra for the sample annealed at 800 °C and exposed to X-rays are given.

As seen from the Figure, the band A4 is present in all three cases, though with different intensities. The band A3 lies within the same wavelengths, but immediately after X-ray exposure, it acquires a well pronounced maximum at 1.89 μm and the peak of the band A2 becomes smoothed. Four days after exposure the spectrum takes its initial shape, retaining high intensity.

Fig. 5 illustrates the X-ray intensity dependencies of the short-circuit currents in the p-n structures obtained under different implantation and annealing conditions.

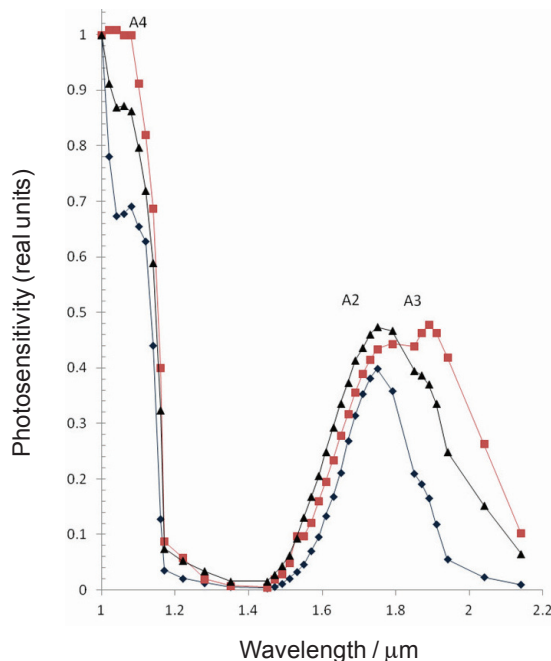


Figure 4. Photosensitivity spectra for the sample annealed at 800 °C ( $10^{14} \text{ cm}^{-2}$ ) before and after X-ray exposure: ♦, before; ■, immediately after; ▲, four days after exposure.

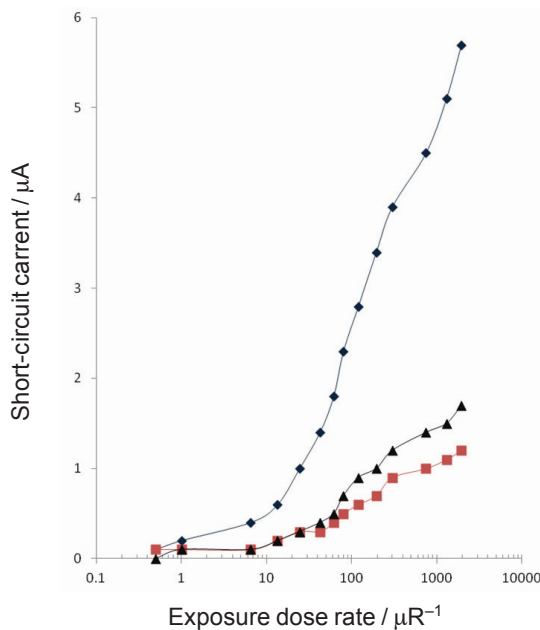


Figure 5. Influence of X-ray radiation on the short-circuit current in p-n junctions obtained under different implantation and annealing conditions: ♦,  $10^{14} \text{ cm}^{-2}$  pulse photon annealing (PPA) for 6 s at 1000 °C; ■,  $10^{14} \text{ cm}^{-2}$ , annealing for 20 min at 800 °C; ▲,  $10^{13} \text{ cm}^{-2}$ , annealing for 20 min at 1000 °C.

As seen from Fig. 5 the PPA structures exhibit the highest sensitivity to X-rays.

It should be noted that the structures implanted with doses of  $10^{14} \text{ cm}^{-2}$  and  $7.8 \times 10^{14} \text{ cm}^{-2}$  and annealed at  $1000^\circ\text{C}$  are practically insensitive to X-radiation.

According to the results of these studies, with a sufficient degree of confidence we can state the following:

- Under the given implantation conditions (three II doses) and at annealing temperatures of  $800$ ,  $900$  and  $1000^\circ\text{C}$  at least three types of defects, responsible for the bands A2, A3 and A4, are formed;
- The closely spaced bands A2 and A3 may correspond to different types of deep-level defects present at all doses and annealing temperatures. The action of X-radiation on the band A3 indicates the metastable character of the defects engendered by certain implantation and annealing conditions; the defects are then transformed to stable ones with increasing dose and temperature or duration of thermal treatment;
- Proceeding from the band intensity, the defects responsible for the bands A2 and A3 have rather a high dose-dependent concentration in the material;
- At the thermal treatment at  $800^\circ\text{C}$  there occurs additionally a type of defect responsible for the band A4, which is fully annealed at  $900^\circ\text{C}$ .

As for the nature of the defects determining the optical properties of the structures in the IR region and the results of X-ray irradiation, we can only make reasonable assumptions that should be independently verified by other methods. We proceed from the fact<sup>13</sup> that during the implantation of B in n-Si with a dose of  $10^{13} \text{ cm}^{-2}$  and an energy of 50 keV no extended defects such as dislocation loops were observed. Therefore, bands A2 and A3 on the IR spectrum are, rather, associated with clusters/nanoformations in the silicon matrix. Here, the complexes responsible for the band A3 (probably in the form of multicharge formations) transfer from a metastable to a stable state, thus changing the electron configuration. As for the band A4, according to the literature it may well correspond to the {113} defect.<sup>7</sup>

Of course, the above defects do not exclude the presence of other types of defects in the ion-implanted material, which either do not participate in the process of absorption at all, or whose photoresponse lies in another spectral region.

A very interesting result was obtained during irradiation of the samples within the wavelengths of  $0.2$ – $0.7 \mu\text{m}$  (UV+vis) and then in the  $0.2$ – $0.4 \mu\text{m}$  UV region. In Table 1 the data for short-circuit current densities in the UV region for the two types of samples are given. They reveal a sufficiently high sensitivity of the samples to UV radiation irrespective of the annealing temperature. The important result is that the UV photosensitivity is more than 60% of the integral sensitivity upon UV+vis irradiation. It can be reasonably assumed that such an outcome is determined by nanostructures (in the form of nanoclusters or ultrashallow p–n junctions) located in the surface layer of the structure and having a larger band gap than that of silicon.

The advantages of the  $1.4$ – $2.0 \mu\text{m}$  spectral region are:<sup>20,21</sup> the transparency of the atmosphere increases markedly, and the brightness of the atmospheric haze is reduced by

<sup>20</sup> N.F. Koshavtsev, A.N. Koshavtsev, C.F. Fedorova. Analysis of the prospects of night-vision device development. *Appl. Phys.*, vol. 3, p. 66, 1999.

<sup>21</sup> M.H. Ettenberry, M.J. Cohen, G.H. Olsen, J.J. Kennedy. InGaAs focal plane arrays and cameras for man-portable near infrared imaging. *SPIE*, vol. 3701, p. 225, 1999.

Table 1. Sensitivity of the samples to UV radiation.

No	Ion-implanted material	Current density $I_1/\mu\text{A cm}^{-2}$ under UV irradiation	Current density $I_2/\mu\text{A cm}^{-2}$ under UV+vis irradiation	$I_1/I_2$ , %
1	Dose $10^{14}\text{ cm}^{-2}$ , annealing temperature $800^\circ\text{C}$ (20 min)	78.0	127.5	61
2	Dose $10^{14}\text{ cm}^{-2}$ , annealing temperature $1000^\circ\text{C}$ (20 min)	71.4	112.2	64

more than an order of magnitude;<sup>20</sup> the use of devices to detect hidden objects is very effective;<sup>21</sup> sensor systems, unlike imagers, may operate in complex meteorological conditions (rain, fog, etc.).<sup>22</sup>

The creation of UV photodiodes with reduced sensitivity in the visible region, allowing one to reduce the influence of background light, is a challenging task. Our results are preliminary and far from being complete. Nevertheless, a large ratio of the UV to UV+vis photoresponses gives hope for further positive practical results.

#### 4. Summary and conclusions

1. The effect of B-implantation dose ( $1 \times 10^{13}$ – $7.8 \times 10^{13}\text{ cm}^{-2}$ ) at an energy of 50 keV and at different annealing temperatures ( $800$ ,  $900$  and  $1000^\circ\text{C}$  for 20 min) in commercial n-Si substrates on the photosensitivity spectra in the near-infrared range ( $1$ – $2.2\text{ }\mu\text{m}$ ) and on the short-circuit current under UV irradiation ( $0.2$ – $0.4\text{ }\mu\text{m}$ ) as well as the action of X-rays from a Co source has been studied.

2. It is shown that in the IR range, in addition to the photosensitivity band A1 associated with the band-to-band absorption in Si, in all cases there appear two other well-defined bands: A2 with a peak at  $1.73\text{ }\mu\text{m}$ , and A3 with a smoothed peak in the range of  $1.45$ – $2.14\text{ }\mu\text{m}$ . At  $800^\circ\text{C}$  another band A4 with a peak at  $1.08\text{ }\mu\text{m}$  appeared.

3. The sensitivity to the change in the X-ray intensity is observed only in the structures obtained either with a low dose ( $10^{13}\text{ cm}^{-2}$ ) or annealed at  $800^\circ\text{C}$  with PPA for 6 s.

4. It is assumed and substantiated that extended defects cannot be responsible for the behaviour of the A2 and A3 bands in the IR spectra, but rather are clusters (nanostructures) existing in the p–n structures in large quantities. The band A4 may be determined by {113} defects.

5. A sufficiently high photosensitivity to UV radiation in the range of  $0.2$ – $0.4\text{ }\mu\text{m}$ , constituting over 60% of the integrated sensitivity (UV + visible), is demonstrated. It is proposed that this result is due to nanostructure formations (such as quantum dots or ultrashallow p–n junctions) with a band gap greater than that of silicon and located in the surface layer of the structure.

6. The high photosensitivity of the material to one of the most useful IR regions ( $1.4$ – $2.2\text{ }\mu\text{m}$ ) as well as to UV ( $0.2$ – $0.4\text{ }\mu\text{m}$ ) radiation is of practical interest for the development of detecting devices.

<sup>22</sup> V. Aebi, P. Vallianos. Laser-illuminated viewing provides long-range detail. *Laser Focus World*, vol. 36, p. 147, 2000.